Decay of ^{156}Er compound nucleus

B. Fornal,* F. Gramegna, and G. Prete
Laboratori Nazionali di Legnaro, I-35020 Legnaro, Padova, Italy

G. D'Erasmo, E. M. Fiore, L. Fiore, A. Pantaleo, V. Paticchio, and G. Viesti
Istituto Nazionale di Fisica Nucleare and Dipartimento di Fisica dell'Università di Bari, I-70126 Bari, Italy

P. Blasi and F. Lucarelli
Istituto Nazionale di Fisica Nucleare and Dipartimento di Fisica dell'Università di Firenze, I-50125 Firenze, Italy

M. Anghinolfi, P. Corvisiero, M. Taiuti, and A. Zucchiatti
Istituto Nazionale di Fisica Nucleare and Dipartimento di Fisica dell'Università di Genova, I-16146 Genova, Italy

P. F. Bortignon
Istituto Nazionale di Fisica Nucleare and Istituto di Ingegneria Nucleare di Milano, I-20133 Milano, Italy

Ch. Ferrer, G. Nardelli, and G. Nebbia
Istituto Nazionale di Fisica Nucleare and Dipartimento di Fisica dell'Università di Padova, I-35131 Padova, Italy

(Received 25 April 1990)

Charged particles and high energy γ rays from the decay of the ^{156}Er compound nucleus populated at $E_x = 47$ MeV excitation energy by the $^{12}C + ^{144}Sm$ and $^{64}Ni + ^{92}Zr$ reactions have been measured to study possible nonstatistical or entrance channel effects. The experimental spectra and published evaporation residue and neutron data are compared with statistical model calculations. The comparison shows that the statistical model with standard parametrization of level density and yrast lines describes reasonably well the bulk of experimental observables but not the shape of neutron spectra if account is taken of the enhancement factor for $E2$ transitions. The discrepancies between experimental data and model calculations are discussed.

I. INTRODUCTION

Angular momentum distributions for the dominant decay channels of the ^{156}Er compound nucleus (CN) have been recently studied with the Darmstadt-Heidelberg crystal ball in the nearly mass-symmetric ($^{64}Ni + ^{92}Zr$) and asymmetric ($^{12}C + ^{144}Sm$) entrance channels,[1] following an earlier investigation of neutron emission from the $^{64}Ni + ^{92}Zr$ reaction.[2] Strong differences in the αn yield and $2n/3n$ cross section ratio have been observed for ^{156}Er compound nuclei populated at the same excitation energy (47 MeV) and spin with the two reactions. These results were interpreted as entrance channel memory during the decay of the CN. It has been suggested[1,2] that during the relaxation of the shape degree of freedom, nuclei populated via the symmetric channel are trapped in a superdeformed minimum of the potential energy surface that is not reached in the carbon-induced reaction. This hypothesis is also supported by the fact that the experimental data of the $^{64}Ni + ^{92}Zr$ reaction[2-4] cannot be reproduced by statistical model calculations including standard parametrization of nuclear properties. It has been shown that a reasonable account of the experimental observable is obtained by model calculations performed with the computer code CASCADE (Ref. 5) in which an elevated yrast line and a level density parameter $a = A/12$ are used.

The elevated yrast line was supposed to correspond to superdeformed shapes for $A \sim 160$ nuclei which have been recently discovered in gamma-ray studies.[6,7] The inclusion of this line in statistical model calculations follows the suggestion of a trapping of the compound nucleus in a superdeformed minimum. As already discussed in Ref. 4, this is not consistent with the observed properties of the superdeformed bands. These bands are known to become yrast only at quite high spin ($J \geq 50\hbar$) and the strength of their transitions is at most 1% of the fusion-evaporation cross section. The average spin for the decay out of the band is around $J \sim 20\hbar$ with feeding of the oblate yrast band. The use of the elevated yrast line would imply that all nuclei populated in the $^{64}Ni + ^{92}Zr$ reaction are superdeformed independently from the spin, i.e., from the corresponding expected equilibrium shape. In this case the compound nucleus deformation would remain frozen in this shape, being the deformation degree of freedom not relaxed during the particle emission. Phenome-

na related to the dynamics of shape relaxation during particle evaporation or fission have been observed in this mass region,[8] but only for the lifetime of the compound system $\tau \leq 10^{-21}-10^{-20}$ s, much shorter than that of ^{154}Er at 47 MeV excitation ($\tau \sim 8\times 10^{-20}$ s). The use of the level density parameter $a = A/12$ is also rather unusual in this mass region. Systematics of level densities indicate a values in the range $A/7-A/8$ for $A \sim 160$ nuclei.[9] The excitation energy considered here ($E_x = 47$ MeV) is such that a decrease of the level density parameter a caused by temperature effects[10] can be disregarded. Furthermore in a recent experiment[11] the level density parameter was directly measured to be $a = A/8.8$ for the ^{92}Zr(^{64}Ni, $1n$)^{155}Er reaction.

In this paper we report on measurements of charged particles and energetic γ rays emitted in the decay of the compound nucleus ^{156}Er populated in the ^{64}Ni- and ^{12}C-induced reactions. The present experiment was motivated by the well known sensitivity of the spectral shape of charged particles[12] and giant dipole resonance (GDR) strength distribution[13] to the level densities and shapes of nuclei in the deexcitation chain. These experimental data, when linked to the published evaporation residue cross sections and spin distributions, allow a more detailed test of the statistical model predictions for the ^{156}Er, probing also for nonstatistical effects related to the reaction entrance channel.

II. EXPERIMENTAL METHODS AND RESULTS

The experiment was performed at the XTU Tandem facility of the Laboratori Nazionali di Legnaro. 245 MeV ^{64}Ni and 73 MeV ^{12}C beams were used to bombard targets of 0.2 mg/cm^2 ^{92}Zr (96% enriched) and 2 mg/cm^2 ^{144}Sm (90% enriched). Targets were placed at the center of a small, thin walled scattering chamber (30 cm diam, 9 cm height) in which the charged particle telescopes were housed at a distance of 10 cm from the target. Four three element telescopes were used at $\theta_{lab} = 30°$, 60°, 120°, and 150°. The telescopes employed 10–20 μm and 200 μm thick, 50 mm^2 silicon detectors as ΔE_1 and ΔE_2, respectively. Residual energy detectors were 2 cm thick CsI(Tl) scintillators with photodiode readout for the two forward angle telescopes and standard 1 and 2 mm thick silicon detectors for the backward angle ones.

The scattering chamber was placed inside a BaF_2 γ-ray calorimeter which was used to measure sum energy and multiplicity of the γ cascade that follows the particle and/or hard γ emission in the CN deexcitation. The calorimeter was made of 14 individual BaF_2 detectors (hexagonal section of 55 cm^2 surface, 12 cm thick) covering $\sim 80\%$ of the total solid angle. The prompt γ flash in the calorimeter was used as a fast event trigger for charged particle and high-energy γ-ray detectors.

Energetic γ rays were detected at $\theta_{lab} = 110°$ by a 10.2×10.2 cm $Bi_4Ge_3O_{12}$ scintillator, surrounded by a plastic scintillator anticoincidence detector as well as by a 10 cm thick lead shield. Time-of-flight over a 83 cm path was used to separate detected γ rays from neutrons, using the start signal from the BaF_2 calorimeter. Pile up was rejected by an appropriate electronic circuitry.

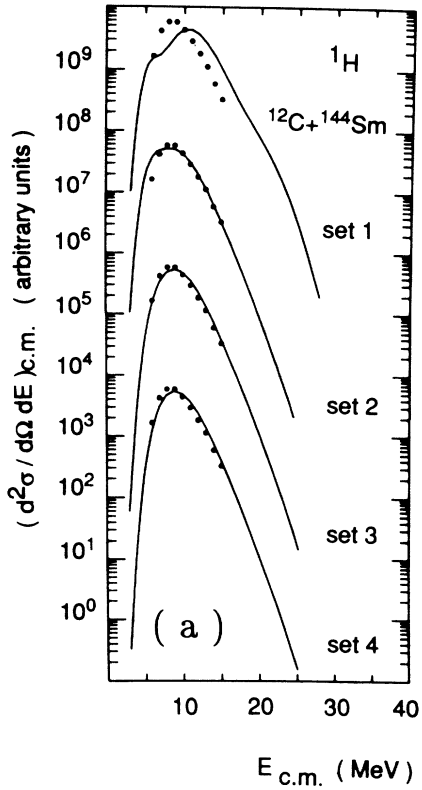

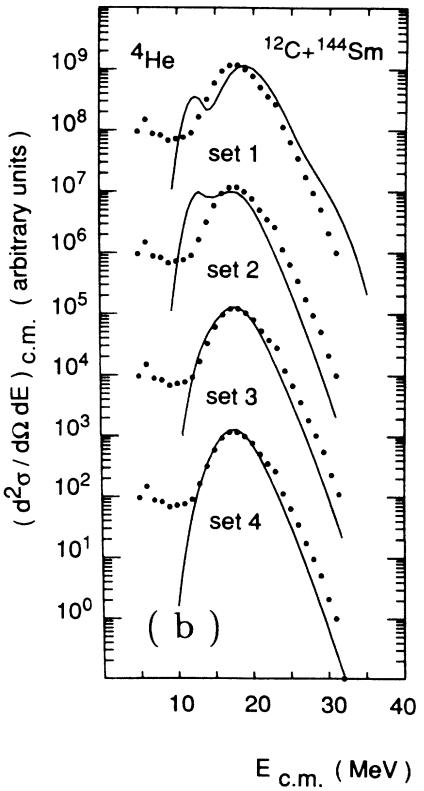

FIG. 1. Center-of-mass converted H (a) and He (b) spectra from the ^{12}C+^{144}Sm reaction measured at $\theta_{lab} = 120°$. Solid lines describe the results of CASCADE statistical model calculations using different input sets.

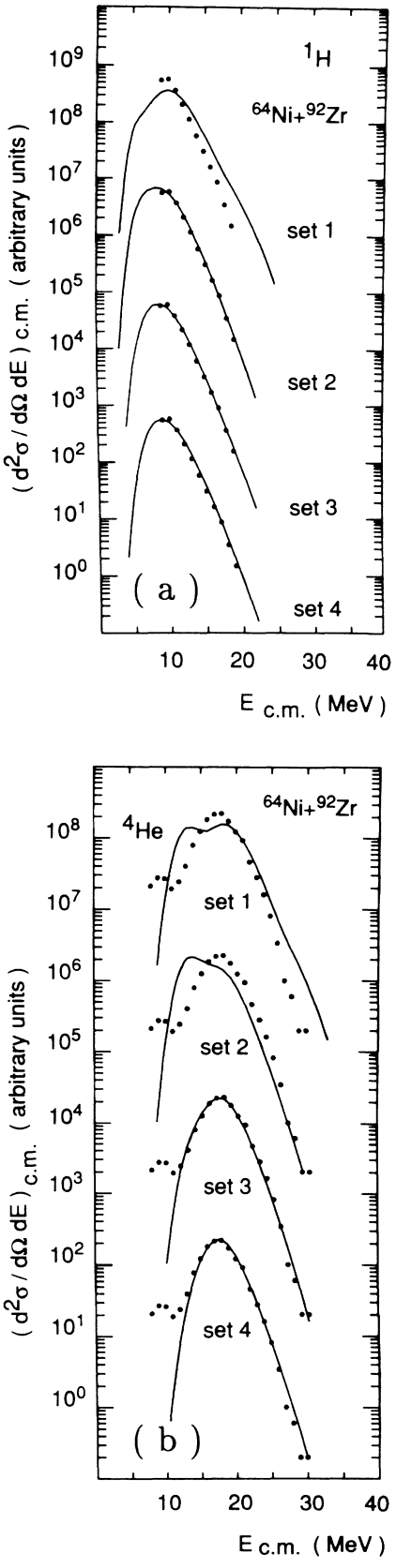

FIG. 2. Center-of-mass converted H (a) and He (b) spectra from the ^{64}Ni+^{92}Zr reaction measured at $\theta_{lab}=120°$. Solid lines describe the results of CASCADE statistical model calculations using different input sets.

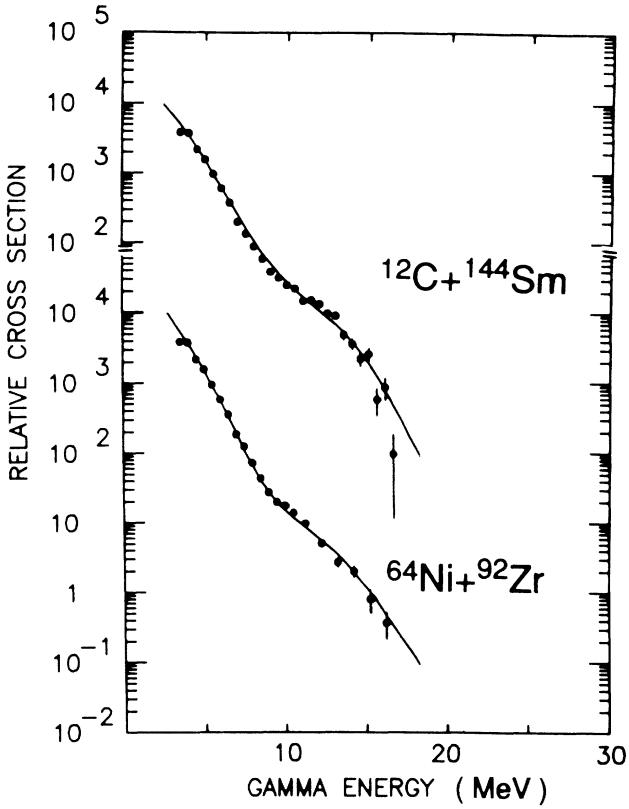

FIG. 3. γ-ray spectra from the ^{12}C+^{144}Sm and ^{64}Ni+^{92}Zr reactions compared with the results of CASCADE statistical model calculations with level density parameter $a = A/8$.

Overall gain stability was monitored with a light emitting diode. Energy calibrations of the γ-ray detectors were obtained *in situ* by using radioactive sources at low energy and the well known ^{12}C$(p,p'\gamma)$ reaction up to $E_\gamma = 15.1$ MeV.

Coincidences between the BaF_2 calorimeter and charged particle telescopes or $Bi_4Ge_3O_{12}$ detector were collected. Proton and α-particle spectra as well as γ-ray spectra were sorted requiring only γ-ray multiplicity measured in the BaF_2 calorimeter $M\gamma > 1$. Charged particle spectra measured at $\theta_{lab}=30°$ and 60° exhibit contributions from reactions other than evaporation from the CN, especially in the ^{12}C+^{144}Sm system. Therefore, only spectra taken at backward angles were used to test the model calculations. Samples of charged particle spectra are shown in Figs. 1 and 2. The measured γ-ray spectra are shown in Fig. 3.

III. STATISTICAL MODEL CALCULATIONS

Experimental data on the decay of ^{156}Er are compared in this section with the statistical model predictions from the computer code CASCADE, often used in the past to compute evaporation residue distributions and particle spectra.[9,14] Light particle spectral shapes, high-energy γ spectra, and the published evaporation residue cross-section and spin distribution for ^{156}Er at excitation energy $E_x = 47$ MeV have been considered for the comparison.

In Table I we detail the parameter values used in CASCADE calculations. Available default options have been used to assign to the inputs the values resulting from published parametrization of nuclear properties. Spin distributions in the entrance channel have been defined using the values of the critical angular momentum J_{max} and diffuseness Δ derived from measured evaporation residue cross sections.[3] These J_{max} values are in agreement with those directly determined from γ-ray measurements.[1,28] The original version of the CASCADE code was modified to include the yrast lines and fission barriers by Sierk,[22] with finite range corrections, replacing the original rotating liquid-drop model (RLDM) values.[23] We made also possible the account of $E1$ transitions through the giant dipole resonance, with the classical energy-weighted sum-rule strength,[13] instead of the original energy-independent strength.

In the first step we have performed calculations using the default values for the energy-independent γ-ray strengths and the following values of the level density parameter: $a = A/12$ (set 1) and $a = A/8$ (set 2). The results are compared with evaporation residue distributions in Fig. 4 and charged particle spectra in Figs. 1 and 2. For a quantitative comparison, in Table II we report the values of the percent deviation between experimental and calculated cross sections. In Table III we also quote the average neutron multiplicity, taking into account the $1n-4n$ cross sections, to be compared directly with the experimental results from Ref. 3.

In Fig. 4 and in Tables II and III, the poor agreement[2,3] is verified between calculated and experimental evaporation residue distribution (especially the ratio between $2n$ and $3n$ cross sections) in the case of the ^{64}Ni-induced reaction. As reported in Ref. 2, better results are achieved in the reproduction of the ^{12}C-induced reaction data by using the level density parameter $a = A/12$ (set 1). This is also confirmed by the corresponding calculated neutron multiplicity values in Table III: the set 1 calculation reproduces well the experimental multiplicity whereas using the level density parameter $a = A/8$ (set 2 input) a large overestimation is observed.

Charged particle spectra offer further information. It is well known that the shape of the particle spectra is determined by the phase space available to a given decay channel and by the access to this phase space. The available space is primarily determined by the level density of the daughter nucleus that defines the high-energy slope of the evaporation spectra. A comparison between model calculation results and experimental data in Figs. 1 and 2 suggests that the level density parameter $a = A/8$ (set 2) gives a better account of the spectral slope than $a = A/12$ (set 1) for both reactions, in apparent contradiction with the results from the evaporation residue distributions. A second important information arises from

TABLE I. Evaporation calculations using CASCADE.

Angular momentum distribution in the compound nucleus:
A ^{64}Ni+^{92}Zr: $J_{max}=46\hbar$, diffuseness $\Delta=4\hbar$.
B ^{12}C+^{144}Sm: $J_{max}=27\hbar$, diffuseness $\Delta=2\hbar$.

Myers, droplet model with Wigner term mass formula (Ref. 15).

Optical potential for emitted particles:
1 Neutrons, Wilmore and Hodgson (Ref. 16)
2 Protons, Perey (Ref. 17)
3 α particles, Huizenga and Igo (Ref. 18)

Level density parameters at low excitation ($E^* \leq 7.5$ MeV)
1 Fermi gas level density formula (Ref. 19) with empirical parameters from Dilg (Ref. 20)
2 Effective moment of inertia $\mathcal{J}=0.85\times\mathcal{J}_{rigid}$.

Level density parameters at high excitation ($E^* \geq 15$ MeV)
1 Fermi gas level density formula (Ref. 19) with parameters from liquid-drop model (Ref. 21).
2 Level density parameter $a_\nu = A/\text{DALDM}$ MeV^{-1}:
Set 1: DALDM=12, set 2–4: DALDM=8

Yrast line:
SUBROUTINE BARFIT, A. J. Sierk, L.A.N.L., Group T9, 1984 (Ref. 22)

Fission:
1 Level density parameter at the saddle point $a_f = a_\nu$.
2 Fission barrier: SUBROUTINE BARFIT, A. J. Sierk, L.A.N.L., Group T9, 1984 (Ref. 22)

γ-decay width (Weisskopf units):
1 $E1$ decay: Set 1,2: $B(E1)=10^{-5}$, set 3,4: $B(E1)=$EWSR.
2 $M1$ decay: $B(M1)=3\times10^{-2}$
3 $E2$ decay: set 1,2: $B(E2)=5$; set 3: $B(E2)=200$; set 4: $B(E2)=500$

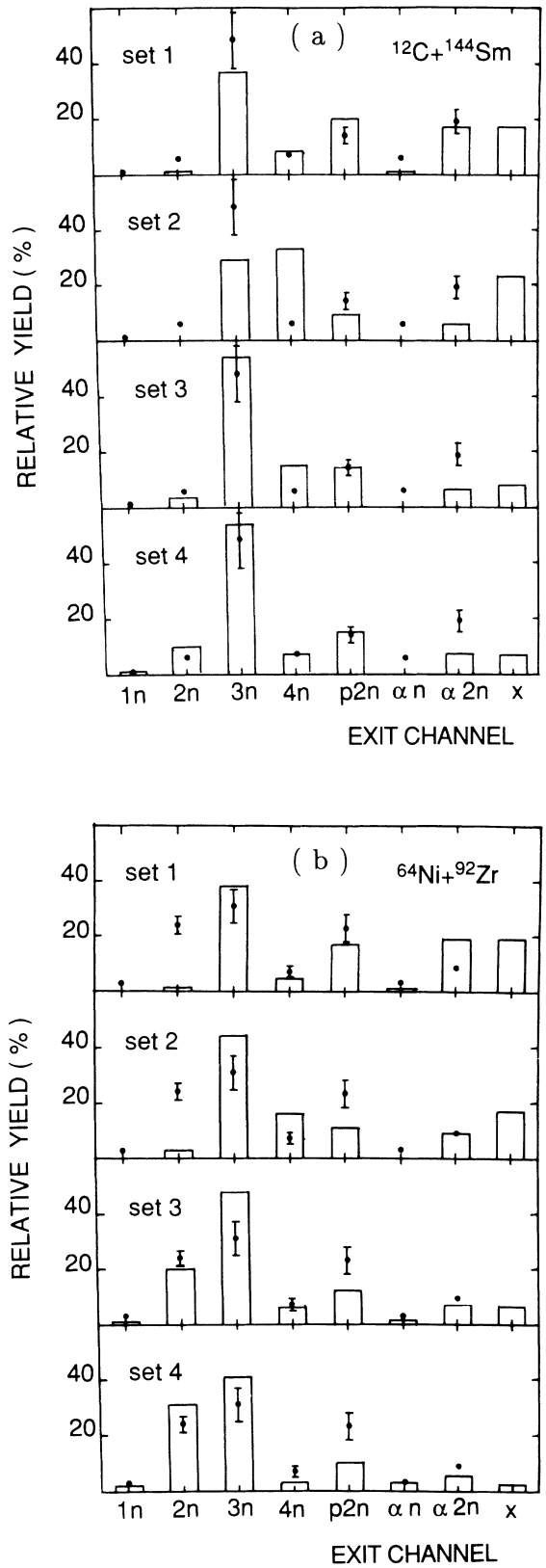

FIG. 4. Experimental evaporation residue distributions (Ref. 1) for the $^{12}C+^{144}Sm$ (a) and $^{64}Ni+^{92}Zr$ (b) reactions compared with the results of CASCADE statistical model calculations using different input sets.

TABLE II. Percent deviation between experimental and calculated evaporation residue cross-section distributions.

	$^{12}C+^{144}Sm$	$^{64}Ni+^{92}Zr$
CASCADE set 1	32%	50%
CASCADE set 2	78%	59%
CASCADE set 3	34%	38%
CASCADE set 4	30%	40%

the low-energy part of the spectra: the calculations largely overestimate the experimental yield for particle energies close to the emission barrier generating a spurious low-energy peak. This extra production by model calculations of low-energy particles in the low-excitation-energy region also influences the number of emitted neutrons and seems to be responsible for the poor reproduction of the experimental evaporation residue data. The particle-gamma competition at low excitation is therefore supposed to be a critical point in the statistical model calculation for ^{156}Er.

A large enhancement [of a factor 200–300 Weisskopf units (W.u.)] for the $E2$ transition rates in the rare earth region is, indeed, well documented experimentally.[24,25] Experimental values are much larger than the value $B(E2)=5$ W.u. contained in CASCADE as a default option and used in calculations with set 1 and 2 input. Superdeformed shapes, as those supposed to be excited in the ^{64}Ni-induced reaction, are characterized by very large $B(E2)$ values ($\sim$2000 W.u.). For this reason we performed calculations using the usual level density parameter value $a=A/8$ and improving the description of the gamma decay. The $E1$ strength was given by the energy-weighted sum rule with GDR excitation and the $E2$ strength was enhanced. Calculations using $B(E2)=200$ and 500 W.u., labeled set 3 and set 4, respectively, are reported in Figs. 1, 2, and 4 and Tables II and III and show, indeed, a much better account of the experimental data. The shape of the charged particle spectra is now described correctly in the low-energy region too, with the disappearance of the spurious low-energy peak. In the calculations with enhanced $E2$ transition rates, the γ decay competes more effectively at low excitation energies, reducing the yield of low-energy particles. The predicted shape of the particle spectra exhibits only a small dependence on the $B(E2)$ values. The disappearance of the spurious low-energy peak in the particle spectra results also in a reduction of the particle decay chain length, i.e., of the neutron multiplicity that de-

TABLE III. Experimental (Ref. 3) and calculated average neutron multiplicity taking into account the $1n-4n$ cross sections.

	$^{12}C+^{144}Sm$	$^{64}Ni+^{92}Zr$
CASCADE set 1	$M_n=3.2$	$M_n=3.1$
CASCADE set 2	$M_n=3.5$	$M_n=3.2$
CASCADE set 3	$M_n=3.1$	$M_n=2.8$
CASCADE set 4	$M_n=3.0$	$M_n=2.6$
Expt. (Ref. 3)	$M_n=3.1$	$M_n=2.6$

creases with increasing gamma decay strength, as shown in Table III. Computed neutron multiplicities (set 3 and set 4) are close to the experimental value in case of the ^{12}C-induced reaction, whereas in the ^{64}Ni case good agreement is reached only with the larger $B(E2)$ value. Looking at the overall comparison between experimental and calculated evaporation residue distributions (Fig. 4 and Table II), one sees also a relevant improvement going from $B(E2)=5$ W.u. (set 2) to $B(E2)=200$ W.u. (set 3), with smaller differences between set 3 and set 4. In the ^{12}C+^{144}Sm case, the same qualitative agreement between model calculation and experimental evaporation residue distribution is obtained with the level density parameter $a=A/8$ and enhanced $E2$ transition rates with respect to that obtained previously by using the unusual value $a=A/12$ without $B(E2)$ enhancement, the latter calculation also producing unrealistic spectra of evaporated charged particles. An acceptable description of the experimental data is obtained by set 3 and 4 calculations also in the case of ^{64}Ni-induced reaction.

We note that the computed yield of the charged particle channels shows still some underestimation with respect to the experimental data. The shapes of the particle spectra are very well reproduced with the exception of the alpha spectra in the ^{12}C+^{144}Sm reaction. This is because the computed spectra are due only to the $\alpha 2n$ channel, while the experimental ones result also from the contribution of the αn channel, weakly populated in the model calculation.

The need of a level density parameter $a \ll A/8$ was established in previous works to reproduce the shape of neutron spectra from the ^{64}Ni+^{92}Zr reaction.[2] Those spectra are characterized by a slope parameter (average temperature) $T\sim 2.4$ MeV at the lower spin. Such high value of the slope parameter cannot be reproduced by model calculations using the usual level density parameter $a=A/8$ which yields spectra of evaporated nucleons with $T\sim 1.6$ MeV. We stress that proton spectra exhibit a slope parameter $T\sim 1.6$ MeV for both ^{12}C+^{144}Sm and ^{64}Ni+^{92}Zr reactions.

By using CASCADE with the set 3 and 4 input, we have also computed the first moments of the evaporation-residue angular momentum distributions. In Table IV model predictions are compared with experimental results from Ref. 1. We note that the calculated values reproduce several features of the experimental data, although the agreement is slightly worse for the ^{64}Ni-induced reaction. We stress that experimental spin distributions have been obtained from the measured gamma-ray multiplicity distributions, without corrections for the angular momentum removed by particle evaporation, supposed to be small.[1] We check that the statistical model[26] predicts that the spin carried by each evaporated nucleon is $\Delta l\sim 0.6\hbar$ and $\Delta l\sim 1\hbar$ in the case of the ^{12}C- and ^{64}Ni-induced reactions. Larger values are predicted in the case of evaporation of α particles, where the removed spin is $\Delta l\sim 2\hbar$ and $\Delta l\sim 6\hbar$, respectively. Corrections for spin removed by particle evaporations should be taken into account in deriving the spin distributions. Furthermore the determination of the average spin in some xn channels of the ^{64}Ni+^{92}Zr reaction by discrete line γ technique[27–29] yielded values larger than that reported in Ref. 1, resulting in a better agreement with the predicted values.

The comparison in Table IV shows that the two $B(E2)$ enhanced values used give an equivalent description of the ^{12}C data, whereas the better fit is obtained in the ^{64}Ni case by the larger $B(E2)$ value.

IV. GAMMA-RAY SPECTRA

It is well known that the strength distribution of the giant dipole resonance built on excited states contains important information on the shape of the compound nucleus.[13] γ-ray strength distributions in the decay of heavier Er compound nuclei have been measured in the past, showing the well-known splitting of the GDR due to deformation.[30] As average parameters for ^{156}Er centroid and width of a single Lorentzian distribution, we expect from systematics $\langle E\rangle=14.7$ MeV and $\Gamma=7.3$ MeV. A visual inspection of the measured spectra in Fig. 3 shows that the statistics in the GDR energy region are quite poor so that a two-Lorentzian parameter search appears to be unrealistic. One-Lorentzian fits to the experimental distributions reported here were used only to check differences in the GDR strength distribution between the reactions studied. GDR parameters were determined by fitting to the experimental γ-ray spectra those calculated by the modified version of the code CASCADE and folded with the detector response function.[13]

We verified that, as reported in Ref. 2, calculations with energy-independent $E2$ strengths with large enhancement [$B(E2)=200$–500 W.u.] yield gamma spectra without a GDR bump, being the resonance

TABLE IV. First moment of the evaporation-residue angular momentum distribution (Ref. 1). CASCADE statistical model calculations are reported with set 3 (set 4) input.

Exit channel	^{12}C+^{144}Sm $(\langle I_{ER}\rangle/\hbar)^{expt}$	$(\langle I_{ER}\rangle/\hbar)^{calc}$	^{64}Ni+^{92}Zr $(\langle I_{ER}\rangle/\hbar)^{expt}$	$(\langle I_{ER}\rangle/\hbar)^{calc}$
$1n$		27 (23)	43±4	51 (48)
$2n$	21±2	23 (20)	32±3	43 (39)
$3n$	18±2	19 (18)	22±2	29 (27)
$4n$	7±1	15 (17)	7±1	18 (17)
$p2n$	21±2	18 (18)	24±2	28 (26)
αn	15±2	23 (20)	34±3	44 (41)
$\alpha 2n$	10±1	18 (18)	12±1	32 (28)

covered by the tail of $E2$ gamma rays. It is well known that the $E2$ strength,[24] as measured in continuum γ-ray experiments, is concentrated in the so-called $E2$ bump located at low energy in the γ spectra, while the higher energies are dominated by $E1$ transitions. For this reason the GDR parameter search was performed considering only the $E1$ contribution in the spectra for $E_\gamma \geq 4$ MeV. The search yields for the ^{64}Ni+^{92}Zr reaction GDR parameters well in agreement with systematics (strength $S=0.91\pm0.04$ times the classical energy-weighted sum rule, $\langle E\rangle=14.5\pm1$ MeV and $\Gamma=7.5\pm1$ MeV and $\chi^2/\nu=4.4$), using a level density parameter $a=A/8$. The same kind of calculation performed for the ^{12}C+^{144}Sm reaction gives results very close for centroid and width but with an unrealistically high strength ($S=1.8\pm0.4$, $\langle E\rangle=15.0\pm1$ MeV, $\Gamma=6.3\pm1.6$ MeV, and $\chi/\nu=3.8$). Aside from the poor reproduction of the GDR line shape, intrinsically connected to the used one-Lorentzian distribution as shown by the poor values for the reduced chi-square χ^2/ν obtained, the main point of this search is the difference in strength obtained for the two reactions, whereas centroids and widths are practically the same within the errors and in agreement with the systematics. Calculations with level density parameters $a=A/12$ give lower values for the resonance centroids ($\langle E\rangle\sim13.5-14.5$ MeV) with a too large width ($\Gamma\sim10$ MeV).

V. DISCUSSION AND CONCLUSIONS

A large set of data is today available for the decay of the ^{156}Er compound nucleus populated via the mass-symmetric ^{64}Ni+^{92}Zr and mass-asymmetric ^{12}C+^{144}Sm entrance channels at 47 MeV excitation energy. The reported difficulties in reproducing the experimental data with statistical model calculations using standard parametrization of nuclear properties, have been taken in the past as evidence for strong deformation effects which show up in the symmetric entrance channel.[2–4] Differences in angular momentum distributions for the relevant decay channels have been measured in the crystal ball and have been interpreted as an entrance channel effect.[1]

We have measured charged particle and energetic γ-ray spectra for the two entrance channels. The comparison of measured charged particle spectra with statistical model calculations yields the following information: (1) The level density parameter $a=A/12$ used in the past in CASCADE calculations for ^{156}Er does not fit the spectral shapes. The usual value $a=A/8$ accounts well for the slope of evaporative spectra, in good agreement with the findings of the direct measurement of level density for the system considered.[11] (2) The calculated spectra with standard parametrization, using both level density parameters $a=A/12$ and $A/8$, show an unrealistic growth of low-energy particle emission, which causes the increase of the average neutron multiplicity. This extra production disappears by enhancing the γ-decay width.

The well-known fact that nuclei in the rare earths region show large enhancement for $E2$ emission[24] motivated the calculations reported here with a standard level density parameter and a large enhancement for $E2$ transitions. Such calculations describe well the shapes of charged particle spectra and the evaporation-residue distributions of both reactions. Least-square fits of energetic γ-ray spectra with standard CASCADE calculations yield GDR parameters generally in agreement with systematics. We still found significant deviations between model calculations and experimental data for the α-particle spectra and GDR strength in the case of the ^{12}C+^{144}Sm reactions. Despite the low bombarding energy (~6 MeV/nucleon), a sizable contribution to the measured quantities from incomplete fusion reactions[31] cannot be ruled out, giving a possible explanation for the deviations observed in this case.

We note that the inclusion of "enhanced collective $E2$ transitions" is stated also in some earlier CASCADE calculations,[2,4] although specific values are not reported making a direct comparison impossible. The $E2$ transition rate enhancement needed to reproduce the data has to be compared with the corresponding quantity, related in statistical model calculations to the adoption of the elevated yrast line characteristic of the superdeformed band. Quadrupole transitions within the superdeformed band are very enhanced due to the large intrinsic quadrupole moment Q_0. The experimentally observed $B(E2)$ rates are of the order of $B(E2)\sim2000$ W.u. In this respect, the value $B(E2)=200-500$ W.u. needed in the calculation is far from that value. Furthermore it is difficult to clearly identify differences in the $E2$ strengths giving the best fit to the experimental data using ^{12}C and ^{64}Ni beams. It seems that differences in predicted quantities by using different $B(E2)$ values are within the limits of uncertainty of the statistical model parameters. Direct measurements of $B(E2)$ rates will help to solve this problem.

While the average neutron multiplicity values are well described by model calculations, the experimental neutron spectra from the ^{64}Ni+^{92}Zr reaction[2] are much harder than the predicted ones which, in turn, give a good account for the proton spectral shape. It seems that a consistent calculation of the available experimental neutron and light charged particle spectra from the ^{64}Ni-induced reaction is not possible using the current models. The differences between the neutron and proton spectra evaporated from ^{156}Er might be due to different structural properties of nuclei populated in the decay chains not accounted for by the average parametrizations contained in the CASCADE calculations. One example of similar effects has been recently reported in the literature:[32] large shifts and changes in the shape of the evaporated protons feeding different bands in the ^{82}Sr nucleus have been observed. This effect cannot be explained by statistical model calculations that exclude specific nuclear-structure effects.

A few more words are needed about the entrance channel effects. By using the two different entrance channels, compound nuclei with different spin distributions are populated at the same excitation energy. The independence hypothesis of the compound nucleus decay implies that the memory of the entrance channel is lost: at a given excitation energy and spin the decay of the com-

pound nucleus populates different branches with the same ratio. In complex decay chains as those considered here, the independence hypothesis does not mean that the first moment of the angular momentum distributions for a given decay channel, derived from the measured γ-ray multiplicity only, should be the same by using the two different initial CN spin distributions. It is evident from Table IV that the extremely different locations in the angular momentum coordinate of the αn channel are well accounted for by the model calculations and cannot be taken as unexpected features related to the entrance channel. On the contrary, the model predicts that the ratio σ_{2n}/σ_{3n} as a function of the spin should be the same for the two reactions, whereas the experimental data show large differences between the two channels (see Fig. 2 in Ref. 1). This effect is clearly out of the statistical picture of the compound nucleus decay, which is able, as shown in this work, to describe several aspects of the ^{156}Er decay. Further experimental work is therefore needed to ascertain clear signatures of entrance channel or nuclear-structure effects not contained in the actual statistical model picture of the compound nucleus decay.

We are indebted to Dr. D. Bazzacco (Padova) for several helpful discussions about the BaF_2 calorimeter and E. Durante (Genova) for the $Bi_4Ge_3O_{12}$ detector.

*Permanent address: Institute of Nuclear Physics, Cracow, Poland.

[1]A. Ruckelshausen *et al.*, Phys. Rev. Lett. **56**, 2356 (1986).
[2]W. Kuhn, P. Chowdhury, R. V. F. Janssens, T. L. Khoo, F. Hass, J. Kasagy, and R. M. Ronninger, Phys. Rev. Lett. **51**, 1858 (1983).
[3]R. V. F. Janssens, R. Holzmann, W. Henning, T. L. Lesko, G. S. F. Stephans, D. C. Radford, A. M. Van den Berg, W. Kuhn, and R. M. Ronningen, Phys. Lett. B **181**, 16 (1986).
[4]F. L. H. Wolfs, R. V. F. Janssens, R. Holzmann, T. L. Khoo, W. C. Ma, and S. J. Sanders, Phys. Rev. C **39**, 865 (1989).
[5]F. Puhlhofer, Nucl. Phys. **A280**, 267 (1977).
[6]P. J. Twin *et al.*, Phys. Rev. Lett. **57**, 811 (1986); M. A. Bentley *et al.*, *ibid.* **59**, 2141 (1987).
[7]G.-E. Rathke *et al.*, Phys. Lett. B **209**, 177 (1988).
[8]D. J. Hinde, H. Ogata, M. Tanaka, T. Shimoda, N. Takahashi, A. Shinohara, S. Wakamatsu, K. Katori, and H. Okamura, Phys. Rev. C **39**, 2268 (1989).
[9]See, for example, R. G. Stokstad, in *Treatise on Heavy-Ion Science*, edited by D. A. Bromley (Plenum, New York, 1985), Vol. 3, p. 83, and references therein.
[10]G. Nebbia *et al.*, Phys. Lett. B **176**, 20 (1986).
[11]S. Henss *et al.*, Phys. Rev. Lett. **60**, 11 (1988).
[12]J. B. Natowitz, Nucl. Phys. **A482**, 171c (1988).
[13]K. Snower, Annu. Rev. Nucl. Part. Sci. **36**, 545 (1986).
[14]See, for example, G. Viesti, B. Fornal, D. Fabris, K. Hagel, J. B. Natowitz, G. Nebbia, G. Prete, and F. Trotti, Phys. Rev. C **38**, 2640 (1988), and references therein.
[15]W. D. Myers, *Droplet Model of the Atomic Nucleus* (IFI/Plenum, New York, 1977).
[16]D. Wilmore and P. E. Hodgson, Nucl. Phys. **55**, 673 (1964); P. E. Hodgson, Annu. Rev. Nucl. Sci. **17**, 1 (1967).
[17]F. G. Perey, Phys. Rev. **131**, 745 (1963).
[18]J. R. Huizenga and G. Igo, Nucl. Phys. **29**, 462 (1961).
[19]D. W. Lang, Nucl. Phys. **77**, 545 (1966).
[20]W. Dilg, W. Schantl, H. Vonach, and M. Uhl, Nucl. Phys. **A217**, 269 (1973).
[21]W. D. Myers and W. J. Swiatecki, Nucl. Phys. **81**, 1 (1966).
[22]A. J. Sierk, Phys. Rev. C **33**, 2039 (1986).
[23]F. Plasil, ORNL ALICE Report ONRL/TM-6054, 1977.
[24]R. M. Diamond and F. S. Stephens, Annu. Rev. Nucl. Part. Sci. **30**, 85 (1980).
[25]D. J. Sarantites, M. Jaaskelainen, R. Woodward, F. A. Dilmanian, D. C. Hensley, J. H. Barker, J. R. Beene, M. L. Halbert, and W. T. Milner, Phys. Lett. **115B**, 441 (1982).
[26]The CASCADE code does not yield estimates for the spin removed by particle evaporation; to this end we used the PACE2 code, revised version of the code PACE, see A. Gavron, Phys. Rev. C **20**, 230 (1980).
[27]D. J. G. Love, P. J. Bishop, A. Kirwan, P. J. Nolan, D. J. Thornley, A. H. Nelson, and P. J. Twin, Phys. Rev. Lett. **57**, 551 (1986).
[28]A. Ruckelshausen, B. Haas, D. Habs, R. F. J. Janssens, T. L. Khoo, W. Khun, V. Metag, D. Schwalm, and R. S. Simon, Phys. Rev. Lett. **58**, 1584 (1987).
[29]D. J. G. Love, P. J. Nolan, and P. J. Twin, Phys. Rev. Lett. **58**, 1585 (1987).
[30]J. J. Gaardhoje, A. M. Bruce, and B. Herskind, Nucl. Phys. **A482**, 121c (1988).
[31]J. Wilczynski, K. Siwek-Wilczynska, J. Van Driel, S. Gonggrijp, D. C. J. M. Hageman, R. V. F. Janssens, J. Lukasiak, R. H. Siemssen, and S. Y. Van der Werf, Nucl. Phys. **A373**, 109 (1982).
[32]D. J. Sarantites *et al.*, Phys. Rev. Lett. **64**, 2129 (1990).